

Top structure function at the LHeC

G.R.Boroun*

Physics Department, Razi University, Kermanshah 67149, Iran

(Dated: November 25, 2014)

The proposed linear and nonlinear behavior for the top structure function at the LHeC is considered. We present the conditions necessary to prediction the top structure function $F_2^t(x, Q^2)$ with respect to the different predictions for the behavior of the gluon at low x .

Heavy quark contributions in leptonproduction are an important subject in quantum chromodynamic (QCD) phenomenology at lower values of Bjorken x . In leptonproduction, the primary graph is the Photon-Gluon-Fusion (PGF) model where the incident virtual photon interacts with a gluon from the target nucleon (Fig.1). Theoretical calculations for producing $q\bar{q}(c\bar{c}$ and $b\bar{b})$ are available for leading order (LO) and next-leading-order (NLO) processes at HERA (Experiments H1 and ZEUS). In deep inelastic scattering (DIS), the kinematical region for the photo production is available at $Q^2 \geq 5 \text{ GeV}^2$. The available data by the experiments H1 and ZEUS cover a range of photon virtuality of $5 \leq Q^2 \leq 2000 \text{ GeV}^2$ and Bjorken scaling variable $0.0002 \leq x \leq 0.05$ [1]. In this framework, the processes $e + p \rightarrow e + c\bar{c}(\text{or } b\bar{b}) + X$ are sensitive to the gluon density in the proton and allows to test its universality. The minimum momentum fraction x_g of a gluon within a nucleon to produce a $q\bar{q}$ heavy quark pair is $x_g > \frac{M_{q\bar{q}}^2}{2M_p k}$, where k is the photon energy in the nucleon rest frame. Thus the gluon momentum fraction $x_g^{q\bar{q}}$ in photoproduction (Fig.1) has this behavior for heavy production samples as $x_g^{t\bar{t}} > x_g^{b\bar{b}} > x_g^{c\bar{c}}$ along with sensitivities to choice of heavy quarks mass.

In recent years, both the H1 and ZEUS Collaborations have measured the charm and beauty components F_2^c and F_2^b of the structure functions at small x [1] that those are directly related to the growth of the gluon distribution at that region. Also authors in Refs. [2-8] show connection between the gluon distribution and heavy (charm and beauty) structure functions at small x . This search for charm and beauty production at HERA emphasis the importance of having a consistent theoretical framework for heavy flavor production in DIS. Within the variable-flavor- number scheme (VFNS)[9-10] the charm and beauty densities arise via the $g \rightarrow c\bar{c}(b\bar{b})$ evolution. In view of the success of the BGF within the VFNS perturbatively, we think that it would be interesting to confront with the top component F_2^t of the structure function at small x in the LHeC project [11-12]. A compari-

son LHeC experiment with HERA experiments (H1 and ZEUS) and fixed target experiments (NMC, BCDMS, E665 and SLAC) is given by in Fig.2 and a brief overview can be find in Ref.11. The LHeC project is an investigation of the possibility of colliding an electron beam from a new accelerator with the existing LHC proton at an ep center of mass energy beyond 1 TeV . The LHeC represents an increase in the kinematic reach of DIS and an increase in the luminosity. However, the BGF model for $t\bar{t}$ production will remain a phenomenological model to be a useful tool for studies QCD at a high gluon density where saturation and other non-linear physics enter in an essential way.

To study the process $ep \rightarrow e(t\bar{t})X$ of the LHeC, that is sensitive to the gluon density in the proton, the key question is about the radiative corrections to the heavy flavor production cross sections that are large. For this reason, the LHeC study with 50 GeV electrons on 7 TeV protons with 50 fb^{-1} luminosity is simulated [11]. The kinematic region accessed at LHeC is $0.000002 < x < 0.8$ and $2 < Q^2 < 100,000 \text{ GeV}^2$.

To estimate the top contribution to the structure function we firstly consider the gluon momentum fraction carried by charm and bottom quarks and then prediction the the top component F_2^t of the structure function. The heavy flavor contributions to the proton/nucleus structure functions at small x are given by

$$F_2^q(x, Q^2, m_q^2) = e_q^2 \frac{\alpha_s(\mu_q^2)}{2\pi} \int_{1-\frac{1}{a}}^{1-x} dz C_{g,2}^q(1-z, \zeta) \times G\left(\frac{x}{1-z}, \mu_q^2\right), \quad (1)$$

where $C_{g,2}^q$ and $G = xg$ are the coefficients functions [2-7,13] and the gluon distribution function. In fact, we assume that the heavy flavor quarks in the proton structure function only arise from gluon splitting $g \rightarrow q\bar{q}$. Here $a = 1 + \xi$ where $\xi \equiv \frac{m_q^2}{Q^2}$ and the default common value for the factorization and renormalization scales is $< \mu_q^2 > = 4m_q^2 + Q^2/2$. The expansion of the gluon distribution at an arbitrary point $z = \alpha$ give us an important equation for obtain the momentum gluon fraction carried by gluon distributions for create one pair heavy flavor as

*Electronic address: grboroun@gmail.com; boroun@razi.ac.ir ; brezaei@razi.ac.ir

follows

$$G\left(\frac{x}{1-\alpha}, \mu_q^2\right) = F_2^q(x, Q^2, m_q^2)/e_q^2 \frac{\alpha_s(\mu_q^2)}{2\pi} I, \quad (2)$$

where $K = 1 + \frac{J}{I}$, $I = \int_{1-\frac{1}{a}}^{1-x} C_{g,2}^q(1-z, \zeta) dz$, $J = \int_{1-\frac{1}{a}}^{1-x} (z-\alpha) C_{g,2}^q(1-z, \zeta) dz$ and α has an arbitrary value $0 \leq \alpha < 1$ [14-15]. This equation is a direct relation between the gluon distribution at βx (where $\beta = \frac{K-\alpha}{1-\alpha}$) and heavy flavor structure functions (F_2^c, F_2^b and F_2^t) at x value at LO up to NLO analysis. To test the validity and obtained the momentum fraction of the gluon distribution for the top structure function, let us first discuss this ratio for the charm and beauty structure functions. In Table 1 we obtained the parameter α , where describing the fraction of the gluon momentum in BGF processes for heavy flavor production. In this approximation, we use the charm and beauty structure functions obtained by H1 collaboration 2010 [1] and the gluon distribution is usually taken from the GRV, CETQ or MRST parametrizations [13]. In Figs.3 and 4 we observe the behavior of the charm and beauty structure functions with respect to α in average of x values from the H1 data. For any values of these fractional of the momentum, the charm and beauty structure functions have values between $0 < F_2^c < 0.27$ and $0 < F_2^b < 0.022$ with respect to the experimental data respectively. According to the Fig.5, we can find the average of theses momentum fractional as we have $\langle \alpha^c \rangle \approx 0.1$ and $\langle \alpha^b \rangle \approx 0.7$.

Let us determine the predictions for $\langle \alpha^t \rangle$. We know that the top quark can be produced the LHeC from $Wb \rightarrow t$ reactions where the b quark arises from the intrinsic beauty component. But we are interesting to produce top-quark pairs in $\gamma^* p \rightarrow t\bar{t}X$ reactions. The average value α^t have to go to beyond 1 value as can be seen from the ratio of intrinsic beauty to intrinsic top scales as $\frac{m_b^2}{m_t^2} \simeq \frac{1}{1500}$ where the ratio of intrinsic charm to intrinsic beauty scales is $\frac{m_c^2}{m_b^2} \simeq \frac{1}{10}$. But the asymptotic value α is 1 for fractional of gluon momentum, therefore the threshold Bjorken scaling for top pair production reaches to low values of x at fixed Q^2 (Table 2). In this table, we observe that as Q^2 increase, the initial threshold for the Bjorken scaling for $0 < \alpha < 1$ increases. In Fig.6 we show our predictions for the top structure function F_2^t according to the Bjorken scaling threshold as a function of α at Q^2 and x constant values. We can observe that top structure functions increase as Q^2 increase and x decreases. But with respect to the average α for charm and beauty, we expect that $\langle \alpha^t \rangle \rightarrow 1$. Therefore we choose this expanding point for top pair production to be $\simeq 0.95$. As Fig.7 shows, the NLO predictions for the top structure function are rather stable for Q^2 of order of m_t^2 at low- x values under the renormalization scale with respect to the luminosity. At that expanding point, the top structure functions obtained as a function of x for $Q^2 = 10, 100, 1000$

and 10000 GeV^2 . We observe that the initial point of x increase as Q^2 increases. This value has a maximum at $x \sim 0.2$ when Q^2 increase to 100000 GeV^2 , but this maximum point can be increase toward 0.8 when the expanding point decreases toward 0. With respect to the luminosity in the LHeC, we have expect that the available data to be over a wide small- x range. Thus one can better explore the small- x region where non-linear evolution is required as $\ln 1/x$ terms in the evolution become important [16-17] and where resummation approaches may be required [18]. The main characteristic of this nonlinear evolution equation is that it predicts a saturation of the gluon distribution at very small x , which the recombination processes such as $gg \rightarrow g$, leading to non-linear evolution equation. This saturation effects may be applied to the top structure function at very small x values, which may be possible by studying the very small x region at somewhat larger Q^2 at the LHeC. Now we predict the saturation effects to the top structure function $F_2^t(x, Q^2)$ in the LHeC kinematic range. This picture allows us to write the GLRMQ [19] equation for the gluon structure function at small x as follows

$$\begin{aligned} \frac{\partial G(x, Q^2)}{\partial \ln Q^2} &= \frac{\partial G(x, Q^2)}{\partial \ln Q^2} \Big|_{DGLAP} \\ &- \frac{\gamma \alpha_s^2(Q^2)}{R^2 Q^2} \int_x^1 \frac{dz}{z} [G(\frac{x}{z}, Q^2)]^2. \end{aligned} \quad (3)$$

The factor γ found to be $= \frac{81}{16}$ for $N_c = 3$, and the first term in the r.h.s. is the usual linear DGLAP term in DLLA and the second term is nonlinear in gluon density. Here R is the correlation radius between two interacting gluons and πR^2 is the target area where gluons inhabit. The value of R depends on how the gluon ladders couple to the proton, or on how the gluons are distributed within the proton. R will be of the order of the proton radius ($R \simeq 5 \text{ GeV}^{-1}$) if the gluons are spread throughout the entire nucleon, or much smaller ($R \simeq 2 \text{ GeV}^{-1}$) if gluons are concentrated in hot-spot [20] within the proton. This nonlinear evolution equation can be solve for the nonlinear gluon distribution behavior by some methods as those are presented in Refs.[21,22]. Recently, a general solution of the gluon density was performed in the non-linear evaluation equation kinematical region [23], as the gluon distribution in terms of the initial condition can be expressed by

$$\begin{aligned} G(x, Q^2) &= [G(x, Q^2)|_{Linear-DGLAP}] - \int_x^1 G^2(z, Q_0^2) F e^Y \\ &\times BesselI(0, 2\sqrt{U} \sqrt{\ln \frac{z}{x}}) \frac{dz}{z}, \end{aligned} \quad (4)$$

where

$$\begin{aligned} G(x, Q^2)|_{Linear-DGLAP} &= e^{\eta(Q^2)} [G(x, Q_0^2) + \int_x^1 G(z, Q_0^2) \times \\ &\frac{\sqrt{\zeta}}{\sqrt{\ln \frac{z}{x}}} BesselI(1, 2\sqrt{\zeta} \sqrt{\ln \frac{z}{x}}) \frac{dz}{z}]. \end{aligned} \quad (5)$$

Here $\eta(Q^2) = \int_{Q_0^2}^{Q^2} \frac{1}{\ln \frac{Q^2}{\Lambda^2}} d\ln Q^2$ and $\zeta \equiv \frac{12\eta(Q^2)}{\beta_0}$, other parameterizes can be find in Ref.[23]. Also $\chi = \frac{x}{x_0}$, where $x_0 (= 0.01)$ is the boundary condition that the gluon distribution joints smoothly onto the unshadowed region.

Fig.8 represent our prediction results for the top structure function nonlinear behavior for $R = 5 \text{ GeV}^{-1}$ at $Q^2 = 10000 \text{ GeV}^2$. This result shows that the top structure function behavior is tamed with respect to nonlinear terms at the GLR-MQ equation. The differences are not large for $1E - 5 < x < 1E - 2$ but these differences are more concretely for $1E - 7 < x < 1E - 5$. It shows that screening effects are provided by a multiple gluon interaction, which leads to the nonlinear terms in the DGLAP equation. For $x < 1E - 7$, the nonlinear behavior shows that the top structure function fall deeply to ward negative values. May be the Pomeron amplitude have to fixed to the top structure function at this region.

In conclusion, we prediction the top structure function at the LHeC project at low x and high Q^2 values. At low x we expected that extension of the conventional QCD DGLAP resummation is necessary to explain the data, but the nonlinear behavior tamed deeply at very low x as may be add possible scenarios such as BFKL resummation. We observed that, as x decreases, the singularity behavior of the top structure function is tamed by shadowing effects.

Acknowledgment

Author thanks Thomas Gehrmann for discussions which prompted this study and the Department of Physics of the University of Zurich for their warm hospitality. We are also grateful to A.Cooper-Sarkar for critically reading the manuscript and important comments.

References

1. F.D. Aaron et al. [H1 Collaboration], Phys.Lett.**b665**, 139(2008), Eur.Phys.J.**C65**,89(2010); J. Breitweg et. al., [ZEUS Collaboration], Eur. Phys. J. **C12**, 35 (2000); S. Chekanov et. al., [ZEUS Collaboration], Phys. Rev. **D69**, 012004 (2004); A.Aktas et al. [H1 Collaboration], Eur.Phys.J.**C45**, 23 (2006); Eur.Phys.J.**C40**, 349 (2005).
2. N.N.Nikolaev and V.R.Zoller, Phys.Atom.Nucl**73**, 672(2010); Phys.Lett.B **509**, 283(2001); N.N.Nikolaev, J.Speth and V.R.Zoller, Phys.Lett.B**473**, 157(2000); R.Fiore, N.N.Nikolaev and V.R.Zoller, JETP Lett**90**, 319(2009).
- 3.A.V.Kotikov, A.V.Lipatov, G.Parente and N.P.Zotov, Eur. Phys. J. C **26**, 51 (2002).
4. A.Y.Illarionov, B.A.Kniehl and A.V.Kotikov, Phys. Lett. B **663**, 66 (2008); A. Y. Illarionov and A. V. Kotikov, Phys.Atom.Nucl. **75**, 1234 (2012).
5. N.Ya.Ivanov, and B.A.Kniehl, Eur.Phys.J.**C59**, 647(2009); N.Ya.Ivanov, Nucl.Phys.**B814**, 142(2009); Eur.Phys.J.**C59**, 647(2009)
6. I.P.Ivanov and N.Nikolaev, Phys.Rev.**D65**,054004(2002).
7. N.N.Nikolaev and V.R.Zoller, Phys.Lett. **B509**, 283(2001); Phys.Atom.Nucl.**73**, 672(2010); V.R.Zoller, Phys.Lett. **B509**, 69(2001).
8. G.R.Boroun, B.Rezaei, JETP, Vol.115, No.7, PP.427 (2012); Nucl.Phys.**B857**, 143(2012); Eur.Phys.J.**C72**, 2221 (2012); EPL**100**,41001(2012); Nucl.Phys.A**929**, 119(2014); G.R.Boroun, Nucl.Phys.**B884**, 684(2014).
9. M.A.G.Aivazis, et.al., Phys.Rev.**D50**, 3102(1994).
10. J.C.Collins, Phys.Rev.**D58**, 094002(1998).
11. P.Newman, Nucl.Phys.Proc.Suppl.**191**, 307(2009); S.J.BRODSKY, hep-ph/arXiv:1106.5820 (2011); Amanda Cooper-Sarkar, hep-ph/arXiv:1310.0662 (2013).
12. LHeC Study group, CERN-OPEN-2012-015; F. D. Aaron et al. [H1 and ZEUS Collaboration], JHEP **1001**, 109(2010)[hep-ex/arXiv:0911.0884]; LHeC Study group, LHeC-Note-2012-005 GEN.
13. M.Gluk, E.Reya and A.Vogt, Z.Phys.**C67**, 433(1995); Eur.Phys.J.**C5**, 461(1998); H.L.Lai et. al., [CTEQ Collaboration], Eur.Phys.J.**C12**, 375(2000); A.D.Martin, R.G.Roberts, W.J.Stirling and R.S. Thorne, Eur.Phys.J.**C35**, 325(2004); A.D. Martin, W.J. Stirling, R.S. Thorne and G. Watt, Eur.Phys.J.**C63**, 189(2009).
14. A.M.Cooper-Sarkar et.al., Z.Phys.**C39**, 281(1998); A.M.Cooper-Sarkar and R.C.E.Devenish, Acta.Phys.Polon.**B34**, 2911(2003).
15. G.R.Boroun and B.Rezaei, Eur.Phys.J.**C72**, 2221(2012); JETP **115**, 427(2012).
16. V. Fadin, E. Kuraev and L. Lipatov, Sov. Phys. JETP **44**, 443 (1976); V. Fadin, E. Kuraev and L. Lipatov, Sov. Phys. JETP **45**, 199 (1977); Y. Balitsky and L. Lipatov, Sov. J. Nucl. Phys. **28**, 822 (1978).
17. M. Ciafaloni, Nucl. Phys.B **296**, 49 (1988); S. Catani, F. Fioriani and M. Marchesini, Phys. Lett.B **234**, 339 (1990); S. Catani, F. Fioriani and M. Marchesini, Nucl. Phys.B **336**, 18 (1990); M. Marchesini, Nucl. Phys.B **445**, 49 (1995).
18. G. Altarelli, R. Ball and S. Forte, Nucl. Phys.B **799**, 199(2008).
19. A.H.Mueller and J.Qiu, Nucl.Phys.B**268**, 427(1986); L.V.Gribov, E.M.Levin and M.G.Ryskin, Phys.Rep.**100**, 1(1983).
20. E.M.Levin and M.G.Ryskin, Phys.Rep.**189**, 267(1990).
21. G.R.Boroun, Eur.Phys.J.A **42**, 251(2009).
22. M.Devee and J.K.Sarma, Eur.Phys.J.C **74**, 2751(2014); Nucl.Phys.B **885**, 571(2014).
23. G.R.Boroun and S.Zarrin, Eur.Phys.J.Plus **128**, 119(2013).

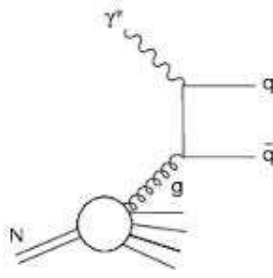


FIG. 1: Boson-gluon-fusion (BGF) graph.

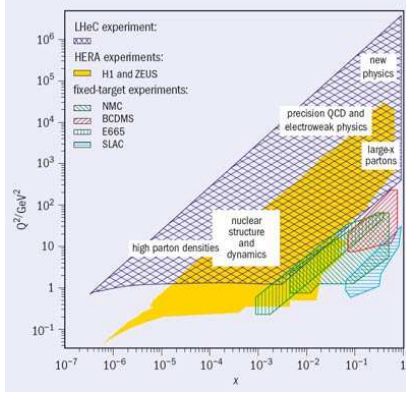


FIG. 2: Kinematic plane for ep collisions in Bjorken- x and resolving power Q^2 showing the coverage of fixed target experiments, HERA and an LHeC.

TABLE I: Values of the gluon momentum fraction (α) with respect to the charm and beauty structure functions (H1 Collaboration.2010 [10]) at the average values of x ($\langle x \rangle$) for $\langle \mu_q^2 \rangle$.

$Q^2(\text{GeV}^2)$	$\langle x \rangle$	$\langle F_2^c \pm \delta \rangle$	α^c	$\langle x \rangle$	$\langle F_2^b \pm \delta \rangle$	α^b
5	0.00020	0.1490 ± 0.010	0.590	0.00020	0.00244 ± 0.010	0.960
8.5	0.00041	0.1815 ± 0.010	0.510	-	-	-
12	0.00073	0.2115 ± 0.010	0.055	0.00056	0.00369 ± 0.011	0.947
20	0.00115	0.2424 ± 0.010	0.013	-	-	-
25	-	-	-	0.00090	0.00896 ± 0.011	0.865
35	0.00182	0.2692 ± 0.011	$\simeq 0$	-	-	-
60	0.00287	0.2772 ± 0.010	$\simeq 0$	0.00315	0.01467 ± 0.010	0.570
120	0.00670	0.2430 ± 0.017	$\simeq 0$	-	-	-
200	0.00900	0.2015 ± 0.028	$\simeq 0$	0.00900	0.01782 ± 0.028	0.410
300	0.01400	0.1975 ± 0.029	$\simeq 0$	-	-	-
650	0.02250	0.1440 ± 0.033	$\simeq 0$	0.02250	0.01210 ± 0.033	0.550
2000	0.05000	0.0600 ± 0.043	$\simeq 0$	0.05000	0.00511 ± 0.043	0.660

TABLE II: The Bjorken scaling initial threshold for top pair production at the LHeC.

$Q^2(\text{GeV}^2)$	$x_0(x < x_0)$
10	0.0001
100	0.0010
1000	0.0100
10000	0.1000

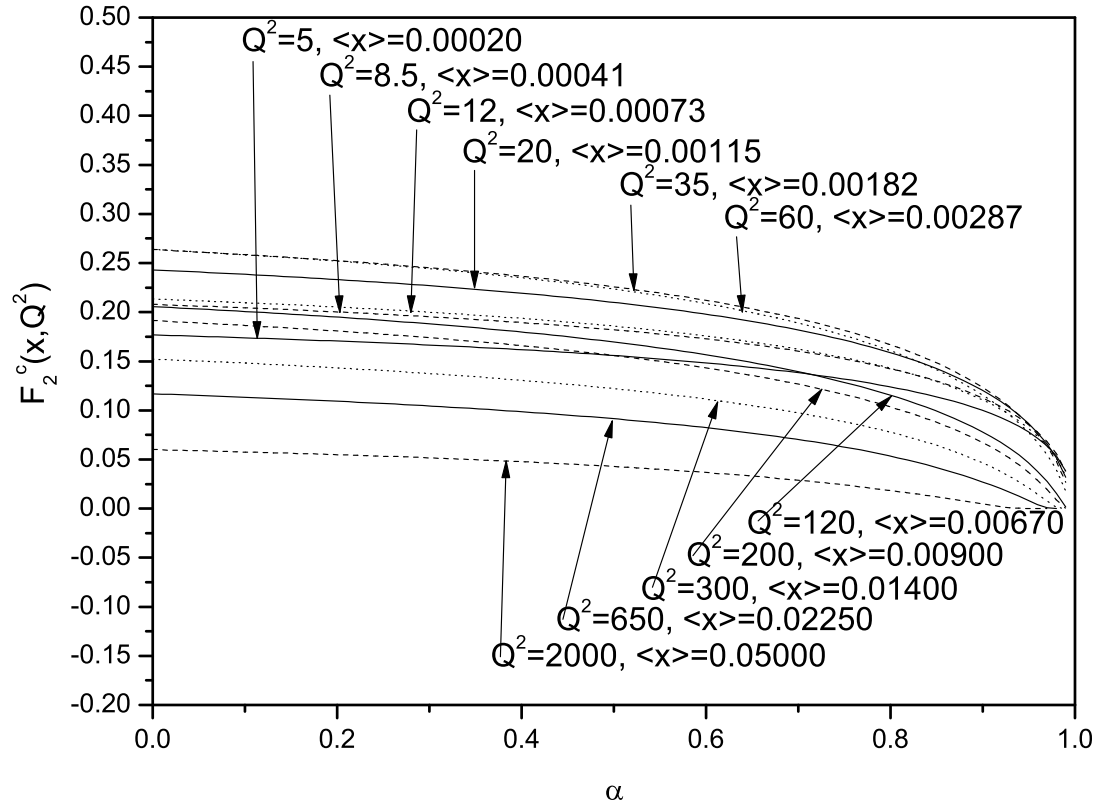


FIG. 3: The charm structure function behavior versus α for the fixed- Q^2 and averages $\langle x \rangle$ values according to the H1 Collab. data (2010)[1].

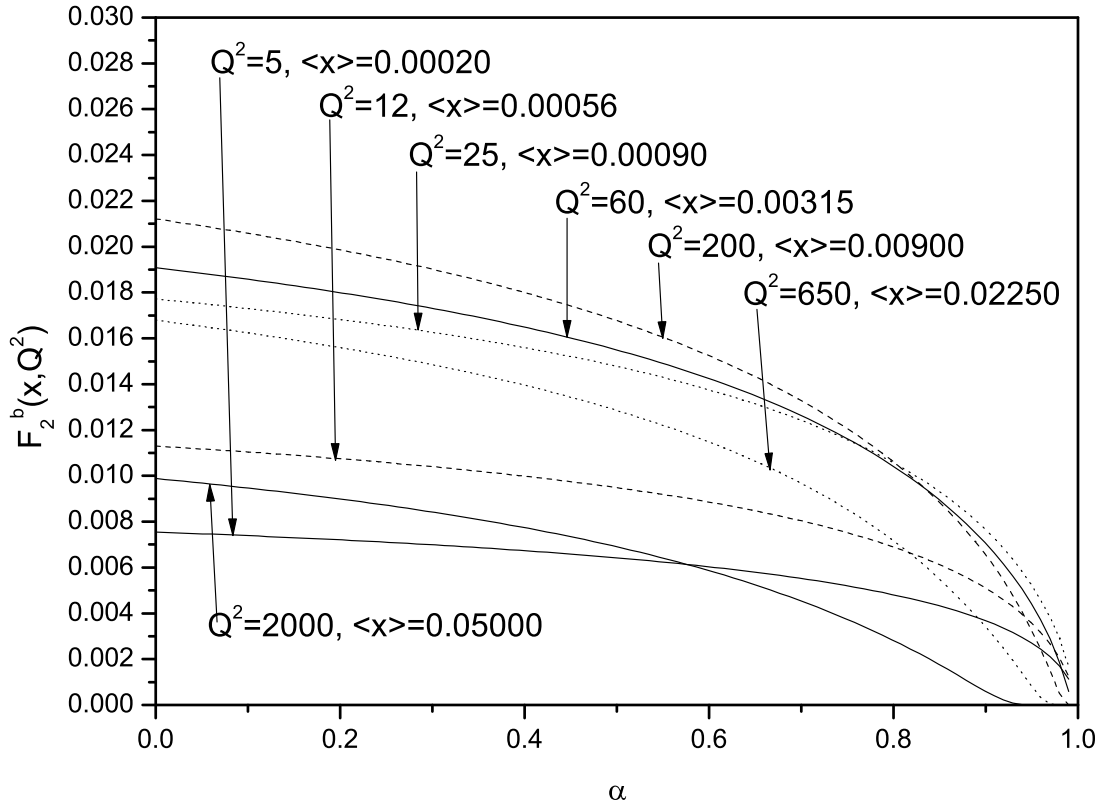


FIG. 4: The beauty structure function behavior versus α for the fixed- Q^2 and averages $\langle x \rangle$ values according to the H1 Collab. data (2010)[1].

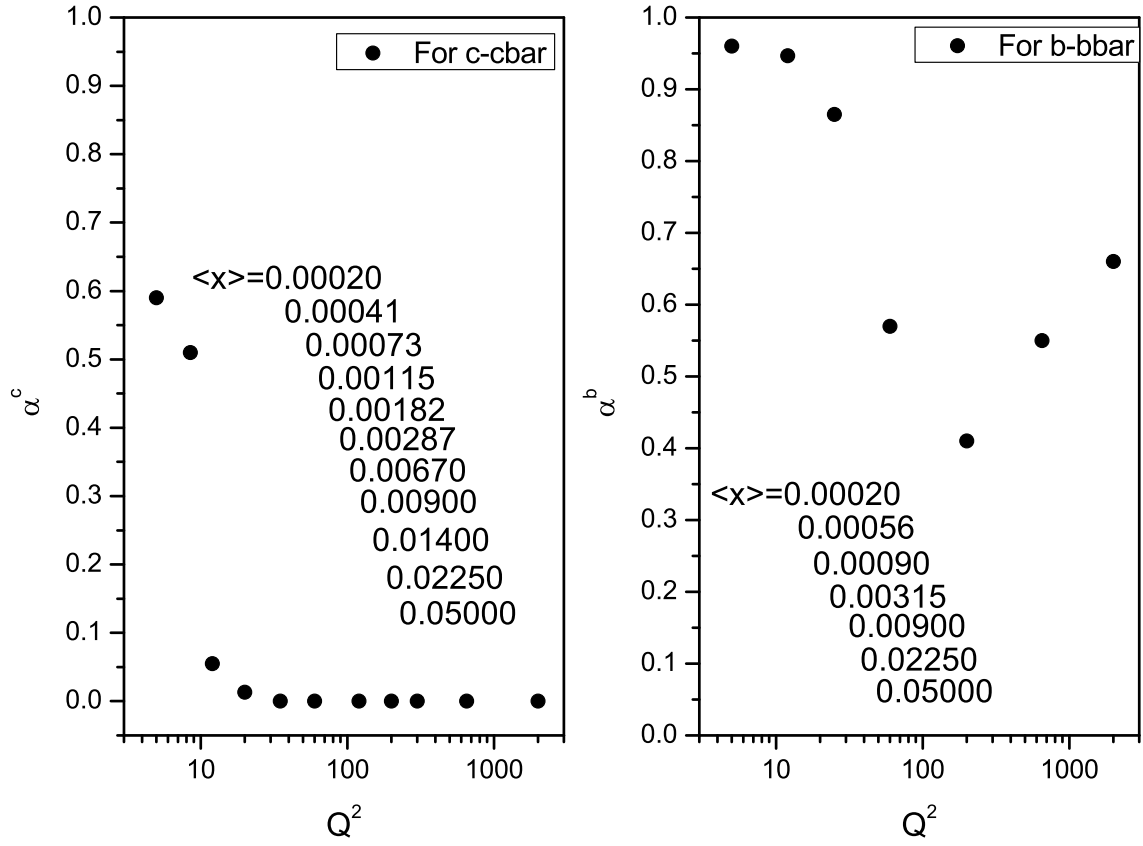


FIG. 5: The expanding point α for the charm and beauty structure functions versus Q^2 at averages $\langle x \rangle$ according to the H1 Collab. data (2010)[1].

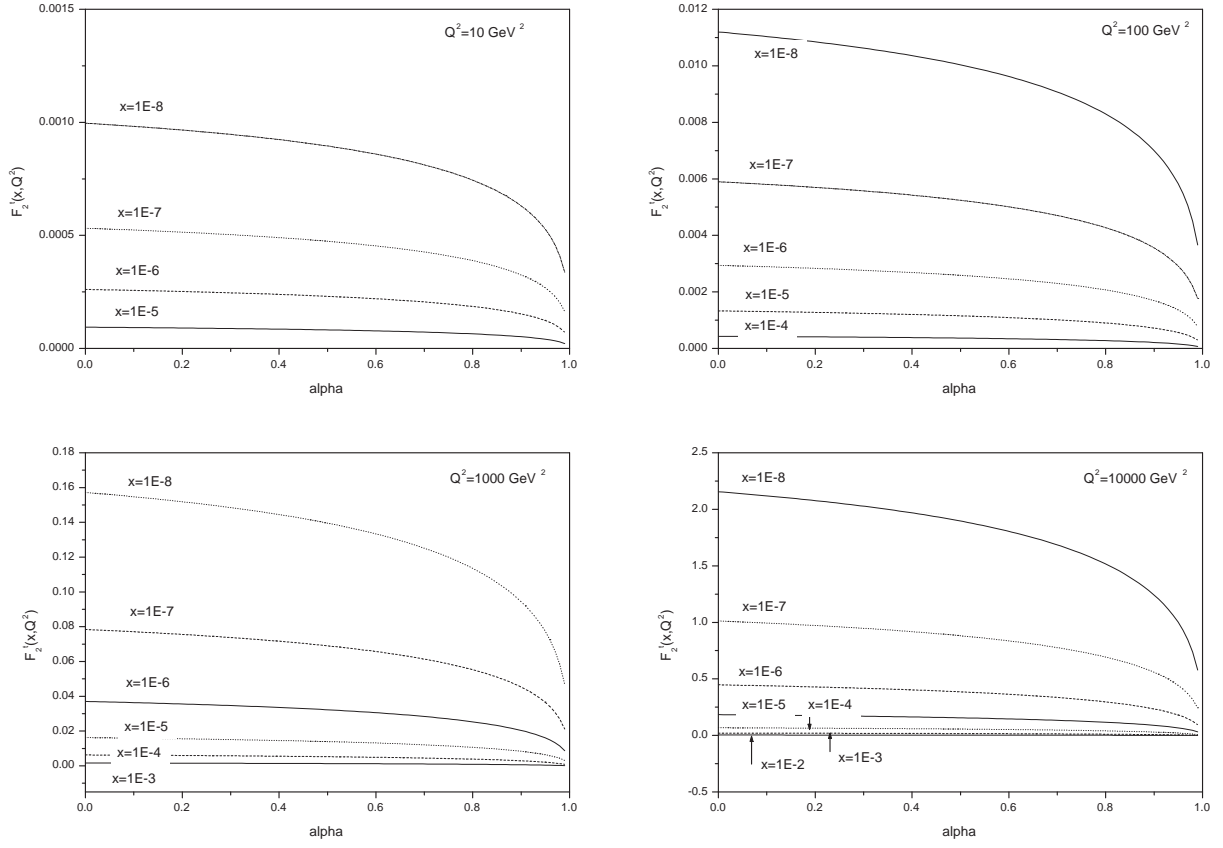


FIG. 6: The top structure function behavior predictions versus α for the fixed- Q^2 .

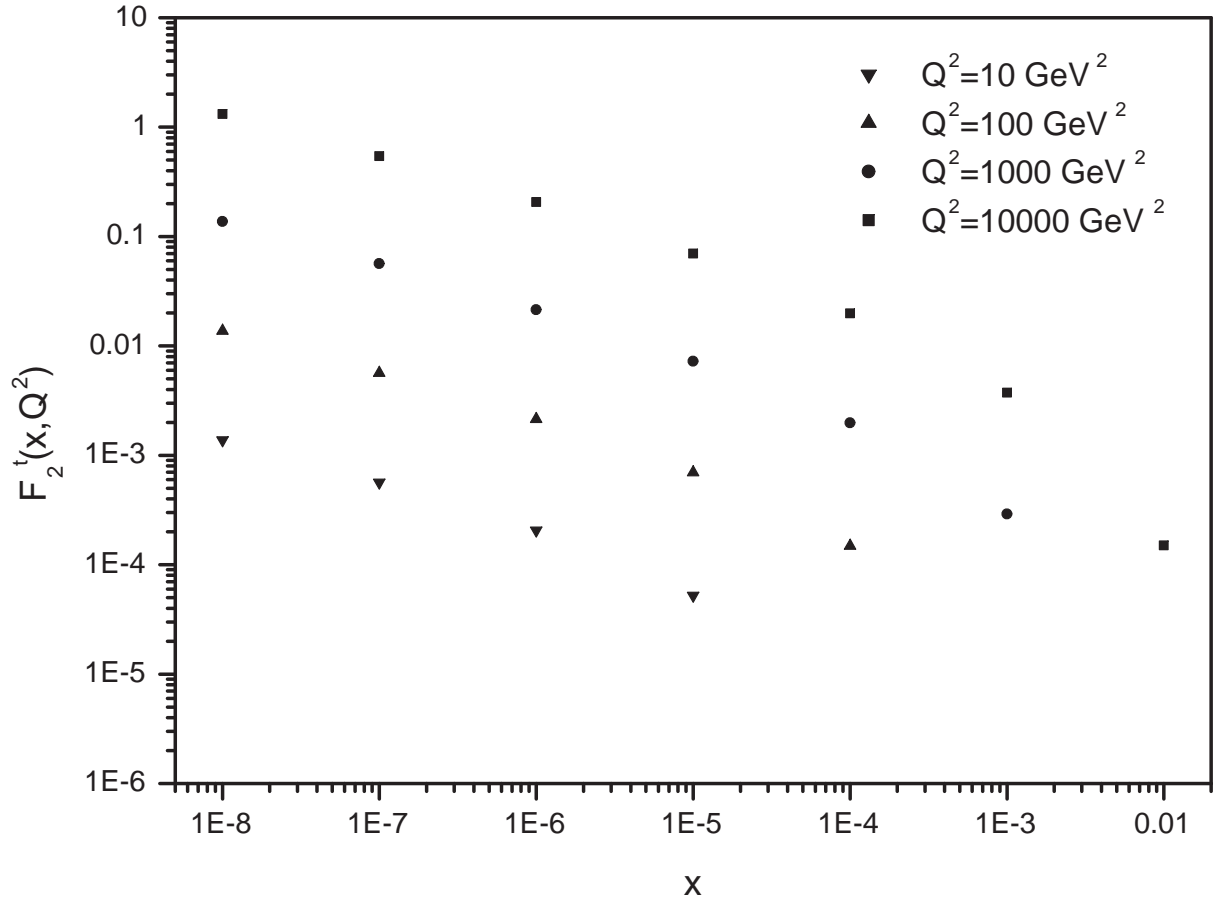


FIG. 7: Our predictions for top structure function in the LHeC for $\alpha = 0.95$ at $Q^2 = 10000 \text{ GeV}^2$.

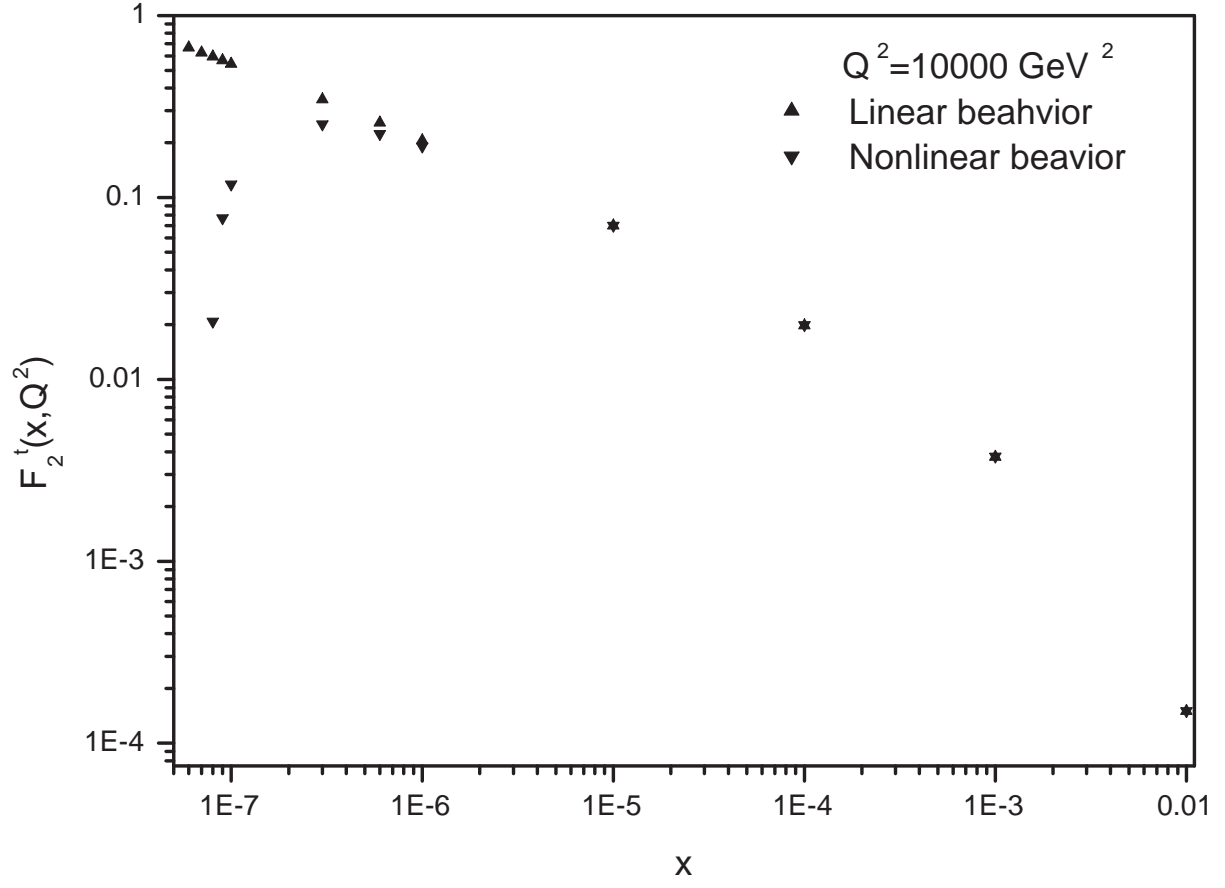


FIG. 8: Nonlinear behavior for top structure function at $Q^2 = 10000 \text{ GeV}^2$.